NJC

Cite this: *New J. Chem.*, 2011, **35**, 2162–2168

www.rsc.org/njc

PAPER

Rhodium(III) and ruthenium(II) complexes of redox-active, chelating *N*-heterocyclic carbene/thioether ligands†‡

Agnès Labande,*[ab] Jean-Claude Daran,[ab] Nicholas J. Long,*[c] Andrew J. P. White[c] and Rinaldo Poli[abd]

Received (in Montpellier, France) 10th March 2011, Accepted 17th May 2011
DOI: 10.1039/c1nj20224c

Half-sandwich rhodium(III) and ruthenium(II) complexes bearing a new redox-active ferrocenyl NHC–thioether ligand have been prepared. The synthesis of ferrocenyl thioether-imidazolium salts **3a** and **3b** was carried out *via* intermediate **2** using an improved procedure. Rhodium(III) complex **4** and ruthenium(II) complex **5** were obtained in good yields and were fully characterised by NMR spectroscopy, X-ray diffraction analysis and electrochemistry. Complex **4** shows a complex ABCD system by ^{1}H NMR, which denotes conformational rigidity due to the presence of several bulky groups. Electrochemical analysis by cyclic voltammetry reveals reversible redox behaviour about the iron centre in **4** and **5**, and indicates electronic communication between iron and rhodium or ruthenium.

Introduction

N-Heterocyclic carbenes (NHCs) have become widely used ligands in many areas from transition metal catalysis,[1] organocatalysis,[2] to biochemistry and medicine.[3] They are generally described as organophosphine analogues, although their σ-donor character is more pronounced. Unlike phosphines, they generally lead to air-stable, robust complexes which do not easily undergo ligand dissociation. However, the M–C bond stability could be detrimental to the catalytic activity. Functionalised *N*-heterocyclic carbene ligands combine the robust nature of the resulting metal–NHC bond with the flexibility of the secondary donor function (hemilability, stereoelectronic control on the active site) and have been successfully used in many catalytic reactions.[4–6] However, any alteration of steric or electronic properties of a ligand implies structural modifications and thus more synthetic work.

Fine-tuning of the electronic properties can also be achieved by introduction of redox-active moieties in the ligands.[7] This has been demonstrated in the field of small molecule sensing[8,9] and in catalysis.[10] In the latter domain, transition metal complexes containing either substitutionally inert [11] or hemilabile [12] redox-active ligands have shown charge-dependent behaviour.

Our group has a strong interest in the chemistry and catalytic activity of functionalised *N*-heterocyclic carbene complexes. We have shown that NHCs bearing thioether or phosphine donors give very efficient and robust catalysts.[13,14] The work reported here describes the preparation of redox-active NHC–thioether ligands incorporating the ubiquitous ferrocene group and the study of their coordination chemistry and electrochemical behaviour.

Results and discussion

Synthesis

The synthesis of the imidazolium salt **3b**, *i.e.* the NHC–thioether precursor, was achieved in three steps from bromoferrocene **1** (Scheme 1). Although the preparation of intermediate **2** and its 1,1′-disubstituted analogue has been described by Mirkin *et al.*,[15,16] we decided to follow a different synthetic route. Mirkin's reported procedures involved the mono-lithiation of ferrocene and afforded the products in very low yields, by reaction with S_8 and tosylate $TsOCH_2CH_2Cl$ (compound **2**, 15% yield),[15] or with disulfide $(ClCH_2CH_2S)_2$ (1,1′-disubstituted analogue, 13% yield).[16] We decided to start from bromoferrocene, which could be selectively and efficiently transformed into lithioferrocene. The reaction of the latter with bis(2-chloroethyl) disulfide was then carried out at

[a] *CNRS, LCC (Laboratoire de Chimie de Coordination), 205, route de Narbonne, F-31077 Toulouse, France. E-mail: agnes.labande@lcc-toulouse.fr; Fax: +33 561553003; Tel: +33 561333158*
[b] *Université de Toulouse, UPS, INPT, LCC, F-31077 Toulouse, France*
[c] *Department of Chemistry, Imperial College London, London, SW7 2AZ, UK. E-mail: n.long@imperial.ac.uk; Fax: +44 2075945804; Tel: +44 2075945781*
[d] *Institut Universitaire de France, 103, bd Saint-Michel, 75005 Paris, France*

† Dedicated to Professor Didier Astruc on the occasion of his 65th birthday.

‡ Electronic supplementary information (ESI) available: Square-wave voltammogram of complex **5**, crystal data and structure refinement and selected bonds and angles for complexes **4** and **5**. CCDC reference numbers 816175 (**4**) and 816176 (**5**). For ESI and crystallographic data in CIF or other electronic format see DOI: 10.1039/c1nj20224c

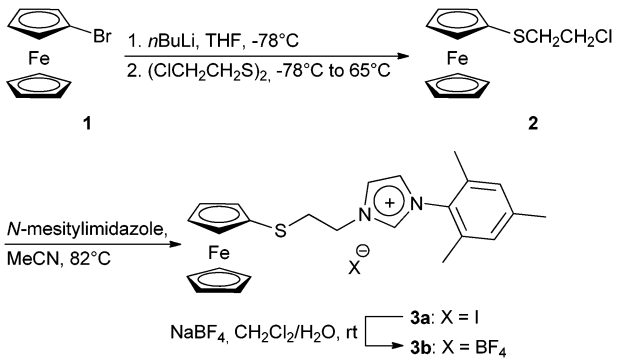

Scheme 1 Synthesis of imidazolium salts **3a** and **3b**.

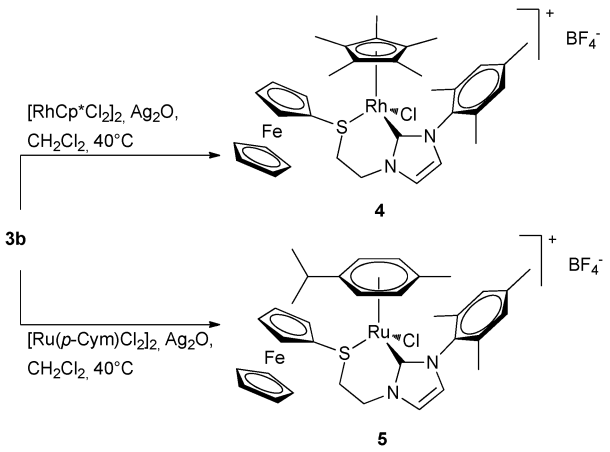

Scheme 2 Synthesis of rhodium(III) and ruthenium(II) complexes.

the THF reflux temperature for 16 h and allowed us to dramatically improve the average yield of **2**, ranging from 70 to 79%.

The intermediate imidazolium salt **3a** was prepared by reaction of **2** with *N*-mesitylimidazole in the presence of NaI to facilitate the substitution (54% yield). This compound was characterised by ^{1}H NMR to confirm the presence of the acidic proton, characteristic of an imidazolium salt, at 9.87 ppm. However, due to the potential hygroscopic nature of salts bearing halogen counter-anions, and to the non-innocent behaviour of these anions in coordination chemistry, a metathesis with $NaBF_4$ was carried out to afford **3b** with an overall yield of 52% from **2**. ^{1}H NMR of **3b** showed the characteristic imidazolium proton signal at 8.78 ppm, shifted upfield relative to **3a**.

The NHC–thioether rhodium(III) and ruthenium(II) complexes **4** and **5** were then prepared by a one-pot synthesis in the presence of Ag_2O as a transmetallating agent (Scheme 2).[6,17] The reaction was carried out with **3b** in order to avoid a potential mixture of Cl and I on the Rh and Ru centres. It was conducted in the presence of excess Ag_2O in dichloromethane at reflux. Forty hours were generally necessary to drive the reaction to completion and consume all the imidazolium salt, as confirmed by the disappearance of the proton signal at 8.78 ppm. The synthesis of silver carbene complexes from imidazolium salts containing non-coordinating counteranions is known but usually requires harsher reaction conditions, such as high temperatures, longer reaction times and the use of molecular sieves, than for those generated from halide-containing imidazolium salts.[18] At least one example describes the use of such silver complexes in transmetallation reactions to prepare Rh(I) complexes.[19] Cationic complexes **4** and **5** were obtained in very good yields (**4**, 86%; **5**, 85%) as deep red and orange solids respectively. Both complexes are air-stable and can be purified by column chromatography on neutral alumina.

Characterisation of complexes 4 and 5

The ^{1}H and ^{13}C NMR spectra of complex **4** confirmed the coordination of both NHC and thioether moieties. The coordination of the carbene on rhodium was evidenced by ^{13}C NMR by a doublet at δ 166.3, with a coupling constant J_{Rh-C} of 54 Hz, typical of rhodium(III)–NHC complexes.[13,14,20] All three methyl groups from the mesityl moiety are now distinct, whereas the two *ortho* methyl groups had the same chemical shift in **3b**. This means that the rotation of the mesityl group along the C–N bond is blocked, presumably because of close contact with the Cp* ligand. The CH_2S signal shifts upfield on going from **3b** (δ 38.1) to **4** (δ 35.2). However, the effects of rhodium coordination were best evidenced by ^{1}H NMR. All the protons of the SCH_2CH_2Im bridge become non-equivalent and appear as a complex ABCD system composed of two doublets of doublets and two doublets of triplets, with the coupling pattern confirmed by a 2D-COSY ^{1}H–^{1}H experiment. This specific pattern is set by the conformational rigidity imposed by the presence of several bulky groups. Indeed, the measured coupling constants are in good agreement with those predicted from the measured dihedral angles from the X-ray structure of complex **4**, allowing us to assign these resonances more precisely as shown in Fig. 1. As in the ^{13}C NMR spectrum, differentiation of the two aromatic protons (slight) and *ortho*, *ortho′* methyl substituents (large) is observed in the ^{1}H NMR spectrum.

The ^{1}H NMR spectrum of the ruthenium complex **5** showed a very different pattern, as all signals were broad even at low temperatures. The formation of the Ru–NHC bond, however, was confirmed by ^{13}C NMR with a signal at δ 164.5, similar to other NHC ruthenium(II) complexes bearing a *p*-cymene substituent.[6] Most signals were assigned by ^{13}C NMR: the

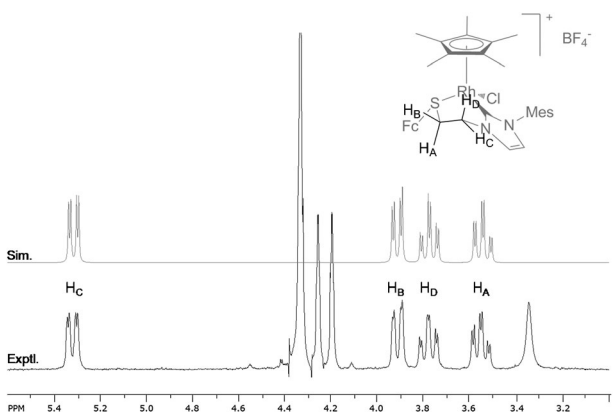

Fig. 1 Assignment of the methylene protons in the ^{1}H NMR spectrum of **4**: ABCD system, simulated (top) and experimental (bottom).

o,*o*′-CH_3 substituents of the mesityl group were barely distinct, whereas both $CH(CH_3)_2$ signals from the *p*-cymene moiety were well separated at δ 20.4 and 24.8. The signals for the CH_2Im carbon appeared in the expected region at δ 49.2, as well as the CH_2S signal at δ 33.7. The ^{13}C NMR signals for ferrocene were situated in the expected region between δ 72 and 68 but appeared very broad. The ^1H NMR spectrum analysis was more complicated. The proton signals of the mesityl and *p*-cymene groups were assigned without ambiguity and all six methyl groups were differentiated. However, only one proton of CH_2Im could be assigned at δ 4.86. The other one was not found even with the help of 2D ^1H–^1H or ^1H–^{13}C correlation experiments, as were the CH_2S protons. Those might be overlapping with other signals, or broadened out. However, the mass spectrometry and X-ray diffraction analyses confirmed the expected structure for **5**.

Complexes **4** and **5** were analysed by single crystal X-ray diffraction.§ Both structures consist of isolated cations and anions with no short interionic contacts. In compound **4**, there is one CH_2Cl_2 solvent molecule. Comparison of selected bond distances, angles and torsion angles are given in Table 1 (also in ESI‡) and ORTEP views for each complex are shown in Fig. 2. The structures are closely related, they both contain the same thioether–NHC ligand chelating the metal to form a six-membered ring and a Cl atom but differ by the π-ligand: Cp* for the rhodium complex and *p*-cymene for the ruthenium compound. The Cp* is in η^5-coordination mode whereas the *p*-cymene is in η^6-coordination. Considering these two ligands as a single coordination site, the overall coordination geometry about each metal centre is pseudo-tetrahedral or typical piano-stool geometry. However, in the case of ruthenium *p*-cymene complexes, it is usual to describe them as pseudo-octahedral, the η^6-ligand occupying one face of the octahedron. The other three sites in complex **5** are occupied by the S1, C5 and Cl1 atoms.

Whatever the description of the coordination about the metal, the M1–S1, M1–C5 and M1–Cl1 bond lengths are comparable for the two compounds (Table 1). The only marked differences concern the angles. Indeed, the Cg1–M1–Cl1 angle is much larger for the ruthenium complex **5**, 125.09(6)°, than for the rhodium one **4**, 119.92(3)°. Such a difference may be explained by the bulkier *p*-cymene ligand with the substituted methyl roughly above the Cl position. Another difference is the larger value observed for the S1–Ru1–C5 angle −91.54(12)° compared to 85.68(5)° for S1–Rh1–C5. This is certainly related to the difference in conformation for the chelate ring, which is boat for the rhodium complex and half-chair for the ruthenium one. The difference is reflected in the S1–C2–C3–N4 torsion angles, −50.5(2)° for **4** and −73.3(4)° for **5**. This difference in conformation results in a different dihedral angle between the coordinated Cp of the ferrocene moiety and the imidazol-2-ylidene ring: 61.03(12)° for **4** and 39.9(2)° for **5**.

Table 1 Selected bond lengths (Å), angles (°) and torsion angle (°) for complexes **4** and **5**

	4 (M = Rh)	**5** (M = Ru)
M1–Cg1	1.8334(8)	1.7460(15)
M1–Cl1	2.3785(4)	2.3944(9)
M1–S1	2.3622(4)	2.3501(10)
M1–C5	2.0550(17)	2.091(4)
S1–C2	1.822(2)	1.798(4)
S1–C18	1.7631(9)	1.774(4)
C2–C3	1.524(3)	1.510(6)
C3–N4	1.459(2)	1.454(6)
C7–C8	1.341(3)	1.331(7)
Cg1–M1–Cl1	119.92(3)	125.09(6)
Cg1–M1–S1	123.28(3)	119.72(6)
Cg1–M1–C5	133.87(6)	134.56(12)
Cl1–M1–S1	90.407(16)	91.66(4)
Cl1–M1–C5	91.64(5)	81.79(11)
S1–M1–C5	85.68(5)	91.54(12)
S1–C2–C3–N4	−50.5(2)	−73.3(4)

Cg1 defines the centroid of the cycle above the metal.

The Rh1–C5 distance of 2.0550(17) Å compares well with related NHC–Cp* rhodium complexes.[20,21] The Ru1–C5 distance of 2.091(4) Å is slightly long but in the range of other NHC–ruthenium complexes, which are found between 2.028(4) and 2.0828(14) Å.[6,21] The average M1–Cl1 and M1–S1 distances are in agreement with other structurally characterised cationic η^5–Cp* rhodium or η^6–*p*-cymene ruthenium complexes reported in the Cambridge Structural Database.[22] Both ferrocene moieties have eclipsed conformation and usual geometry.[22]

Electrochemistry

The imidazolium salts **3a**, **3b** and complexes **4** and **5** were analysed by cyclic voltammetry in dichloromethane. The voltammogram of **3a** exhibited several waves, as the iodide anion itself is redox-active.[23] The redox potential for the ferrocene group is observed at $E_{1/2}$ = +0.64 V/SCE with a chemically reversible behaviour (ΔE_p is 120 mV, however, and may indicate slow electron transfer at the surface of the electrode). The voltammogram of **3b** only shows the chemically reversible wave for the ferrocene unit at +0.64 V/SCE (ΔE_p = 111 mV), see Fig. 3.[24]

The Fe^{II}/Fe^{III} couple in the rhodium complex **4** (Fig. 4) is anodically shifted compared to the imidazolium salts with a potential of +0.77 V/SCE (ΔE_p = 111 mV) and exhibits chemically reversible behaviour. The anodic shift signals a weak electron-withdrawing effect of coordination to rhodium and indicates electronic communication between iron and rhodium through the sulfur atom. The cyclic voltammogram of the ruthenium complex **5** also presents a chemically reversible redox wave at +0.76 V/SCE (ΔE_p = 84 mV) attributed to the

§ *Crystal data for* **4**: $[C_{34}H_{41}ClFeN_2RhS](BF_4)\cdot CH_2Cl_2$, M = 875.69, triclinic, $P\bar{1}$ (no. 2), a = 10.6786(2), b = 11.8064(3), c = 15.8586(3) Å, α = 96.8086(18)°, β = 102.4583(19)°, γ = 106.009(2)°, V = 1842.52(7) Å^3, Z = 2, D_c = 1.578 g cm^{-3}, μ(Mo-Kα) = 1.164 mm^{-1}, T = 173 K, orange tablets, Oxford Diffraction Xcalibur 3 diffractometer; 12 107 independent measured reflections (R_{int} = 0.0239), F^2 refinement, R_1(obs) = 0.0331, wR_2(all) = 0.0856, 10 327 independent observed absorption-corrected reflections [$|F_o| > 4\sigma(|F_o|)$, $2\theta_{max}$ = 66°], 484 parameters. CCDC 816175. *Crystal data for* **5**: $[C_{34}H_{40}ClFeN_2RuS](BF_4)\cdot CH_2Cl_2$, M = 787.92, monoclinic, $P2_1/n$ (no. 14), a = 11.8820(3), b = 10.2423(2), c = 27.5100(7) Å, β = 94.493(2)°, V = 3337.65(14) Å^3, Z = 4, D_c = 1.568 g cm^{-3}, μ(Mo-Kα) = 1.080 mm^{-1}, T = 180 K, orange tablets, Oxford Diffraction Gemini Eos diffractometer; 7574 independent measured reflections (R_{int} = 0.063), F^2 refinement, R_1(obs) = 0.0512, wR_2(all) = 0.1073, 5590 independent observed absorption-corrected reflections [$|F_o| > 4\sigma(|F_o|)$, $2\theta_{max}$ = 55°], 412 parameters. CCDC 816176.

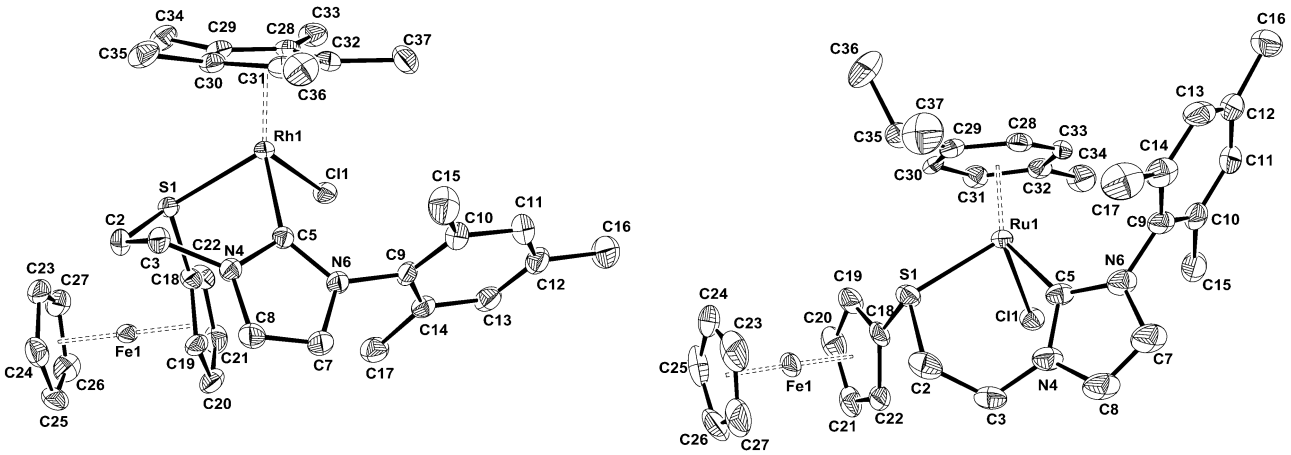

Fig. 2 Molecular views of compounds **4** (left) and **5** (right) with the atom-labelling scheme. Displacement ellipsoids are drawn at the 50% probability level. H atoms have been omitted for clarity.

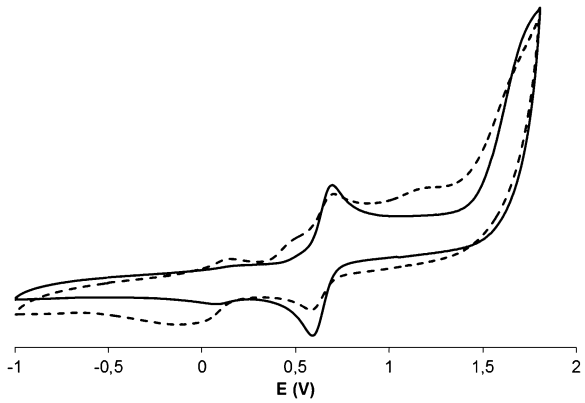

Fig. 3 Cyclic voltammograms of imidazolium salts **3a** (dashed) and **3b** (plain), 1 mM in CH_2Cl_2 at a scan rate of 0.2 V s^{-1}.

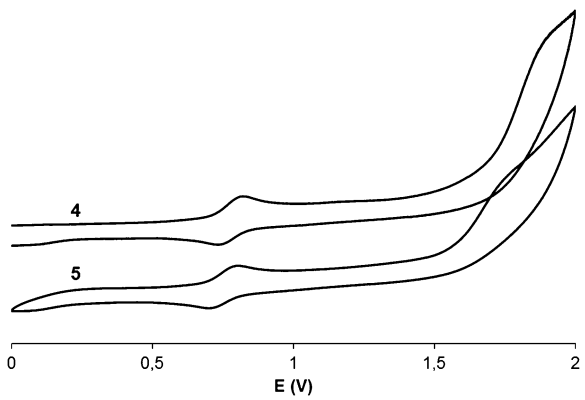

Fig. 4 Cyclic voltammogram of complexes **4** and **5**, 1 mM in CH_2Cl_2 at a scan rate of 0.2 V s^{-1}.

Fe^{II}/Fe^{III} couple, see Fig. 4. A very weak oxidation wave was detected at approximately +1.7 V/SCE and was tentatively assigned to the Ru^{II}/Ru^{III} couple. Analysis by square-wave voltammetry more clearly revealed this wave at +1.68 V/SCE (see ESI‡), however it is far less intense than the Fe^{II}/Fe^{III} wave. A similar Ru(II) *p*-cymene complex, bearing a chelating NHC–thioether ligand with methyl in place of ferrocenyl, exhibits a Ru^{II}/Ru^{III} redox wave at +1.55 V/SCE.[6] The anodic shift of the oxidation potential for the Ru^{II}/Ru^{III} couple is attributed to the stronger electron-withdrawing effect of the oxidised form of ferrocene compared to CH_3. The aspect of the voltammogram also suggests that the iron oxidation has an effect on the redox behaviour of ruthenium, whose oxidation becomes irreversible.[25] The electrochemical behaviour of both complexes suggests that it should be possible to alter selectively and reversibly the oxidation state of iron by a careful choice of oxidizing and reducing agents.[23]

Conclusions

Two half-sandwich rhodium(III) and ruthenium(II) complexes bearing a new redox-active NHC–thioether ligand have been prepared and their electrochemical properties investigated. Cyclic voltammetry experiments have shown that the ferrocenyl unit can be oxidised and reduced reversibly. The catalytic properties of these complexes and the influence of the redox state of iron on the catalytic performances are under investigation and the results will be reported in due course.

Experimental

General procedures

All reactions were performed under an atmosphere of dry nitrogen or argon using standard Schlenk techniques, unless otherwise stated. Solvents were dried and distilled by standard techniques prior to use. NMR spectra were recorded on Bruker AV300, AV400 or AV500 spectrometers. NMR chemical shifts were determined by reference to the residual ^1H or ^{13}C solvent peaks in the deuterated solvents. The NMR simulation experiment was done with SpinWorks 3. Electrospray (ES) mass spectra were recorded either at Imperial College on a Micromass LCT Premier spectrometer or at the Université Paul Sabatier by the Service Commun de Spectrométrie de Masse on a MS/MS API-365 (Perkin Elmer Sciex). Elemental analyses were performed either by Mr Stephen Boyer at London Metropolitan University or by the Service d'Analyses du Laboratoire de Chimie de Coordination in

Toulouse. Cyclic voltammetry (CV) and square-wave voltammetry (SQW) experiments were carried out with a PGSTAT-302N potentiostat (Metrohm) at 20 °C using a Pt disk working electrode, a Pt wire counter electrode and a saturated calomel reference electrode (SCE); a 0.1 M *n*-Bu_4BF_4 solution was used as the supporting electrolyte. All electrochemical data are referenced *versus* SCE. Bromoferrocene **1** was prepared by a previously described procedure.[26]

Syntheses

2-Chloroethylthioferrocene (2)[15,16]. A solution of bromoferrocene (300 mg, 1.13 mmol, containing 92% FcBr, 7% ferrocene and 1% $FcBr_2$) in THF (15 mL) was cooled to −78°C. *n*-BuLi (800 µL, 1.24 mmol) was added dropwise and the solution was stirred for 30 min at −78 °C. A solution of 2-chloroethyldisulfide (260 mg, 1.36 mmol) in THF (5 mL) was added dropwise and the mixture was allowed to warm to room temperature for 2 h. The mixture was then heated at 65 °C for 16 h. It was allowed to cool to room temperature and H_2O (10 mL) was added. The phases were separated and the aqueous phase was extracted with Et_2O. The organic phases were combined, washed with H_2O, dried ($MgSO_4$), filtered and concentrated *in vacuo*. The yellow liquid was purified by column chromatography on neutral alumina (grade I). The first band contained mainly ferrocene and the desired product was obtained as a yellow liquid in the second band (250 mg, 79%). ^{1}H NMR (400 MHz, $CDCl_3$) δ 4.34 (t, J_{HH} = 1.8 Hz, 2H, Cp), 4.26 (t, J_{HH} = 1.8 Hz, 2H, Cp), 4.24 (s, 5H, Cp′), 3.60–3.56 (m, 2H, CH_2Cl), 2.89–2.85 (m, 2H, CH_2S).

1-(β-(Ferrocenylthio)-ethyl)-3-(2,4,6-trimethylphenyl) imidazolium iodide (3a). A mixture of **2** (250 mg, 0.89 mmol), *N*-mesitylimidazole (249 mg, 1.34 mmol) and NaI (267 mg, 1.78 mmol) in degassed acetonitrile (20 mL) was heated at 80 °C for 16 h. After cooling to room temperature, the solvent was evaporated and the residue taken up into CH_2Cl_2. The solution was filtered through Celite and the solvent evaporated to a minimum. Excess Et_2O was added and the yellow precipitate was filtered on Celite, rinsed with Et_2O then taken up into CH_2Cl_2. Evaporation of the solvent afforded **3a** as a yellow solid (268 mg, 54%). ^{1}H NMR (400 MHz, $CDCl_3$) δ 9.87 (t, J_{HH} = 1.5 Hz, 1H, NC*H*N), 7.85 (t, J_{HH} = 1.7 Hz, 1H, *H*C═CH Im$^+$), 7.20 (t, J_{HH} = 1.8 Hz, 1H, HC═C*H* Im$^+$), 7.05 (s, 2H, C*H* Mes), 4.79 (pseudo t, J_{HH} = 5.9 Hz, 2H, CH_2Im$^+$), 4.34 (d, J_{HH} = 1.8 Hz, 2H, Cp), 4.27 (d, J_{HH} = 1.8 Hz, 2H, Cp), 4.20 (s, 5H, Cp′), 3.21 (pseudo t, J_{HH} = 5.9 Hz, 2H, CH_2S), 2.38 (s, 3H, *p*-CH_3 Mes), 2.15 (s, 6H, *o*-CH_3 Mes).

1-(β-(Ferrocenylthio)-ethyl)-3-(2,4,6-trimethylphenyl) imidazolium tetrafluoroborate (3b). Compound **2** (224 mg) was treated as described previously and crude **3a** was dissolved in degassed CH_2Cl_2 (15 mL). A solution of $NaBF_4$ (438 mg, 3.99 mmol) in degassed H_2O (10 mL) was added and the mixture was stirred vigorously for 16 h. The two phases were separated and the aqueous phase was extracted with CH_2Cl_2. The combined organic phases were washed with H_2O, dried (Na_2SO_4), filtered and concentrated *in vacuo* to *ca.* 2 mL. Excess Et_2O was added and the yellow precipitate was filtered through Celite, rinsed with Et_2O, then taken up into CH_2Cl_2. Evaporation of the solvent afforded **3b** as a yellow solid (216 mg, 52%). ^{1}H NMR (400 MHz, $CDCl_3$) δ 8.78 (s, 1H, NC*H*N), 7.73 (s, 1H, *H*C═CH Im$^+$), 7.23 (s, 1H, HC═C*H* Im$^+$), 7.03 (s, 2H, C*H* Mes), 4.48 (t, J_{HH} = 5.9 Hz, 2H, CH_2Im$^+$), 4.33 (d, J_{HH} = 1.7 Hz, 2H, Cp), 4.25 (d, J_{HH} = 1.7 Hz, 2H, Cp), 4.18 (s, 5H, Cp′), 3.07 (t, J_{HH} = 5.9 Hz, 2H, CH_2S), 2.36 (s, 3H, *p*-CH_3 Mes), 2.08 (s, 6H, *o*-CH_3 Mes). ^{13}C NMR (100 MHz, $CDCl_3$) δ 141.36 (C_{quat} Mes), 136.94 (N*C*HN), 134.49 (2 × C_{quat} Mes), 130.64 (C_{quat} Mes), 129.83 (2 × *C*H Mes), 123.70 (*C*═C Im$^+$), 123.52 (C═*C* Im$^+$), 73.94 (2 × *C*H Cp), 69.99 (2 × *C*H Cp), 69.61 (5 × *C*H Cp′), 49.29 (*C*H_2–Im$^+$), 38.07 (*C*H_2S), 21.14 (*p*-*C*H_3 Mes), 17.32 (2 × *o*-*C*H_3 Mes). C_{quat}, Cp not found. ^{19}F NMR (282 MHz, $CDCl_3$) δ −151.6 (BF_4^-). MS (ESI$^+$) *m*/*z* 431 (M$^+$, 100%). Elem. anal. $C_{24}H_{27}BF_4FeN_2S$ (518.03): calc. C, 55.60; H, 5.25; N, 5.41; found C, 55.48; H, 5.28; N, 5.37%.

Rhodium complex (4). Imidazolium salt **3b** (56.4 mg, 0.109 mmol), [RhCp*Cl_2]$_2$ (59.3 mg, 0.096 mmol) and Ag_2O (14.8 mg, 0.064 mmol) were dissolved in dry CH_2Cl_2 (50 mL) and the Schlenk tube was protected from light. The mixture was heated at reflux for 40 h then filtered through Celite and the solvent was evaporated *in vacuo*. The residue was purified by column chromatography on neutral alumina (grade I, deactivated with 6–8% H_2O; eluent: CH_2Cl_2/MeOH 95 : 5) to give a deep red solid (74 mg, 86%). X-Ray quality crystals were obtained by slow diffusion of cyclohexane in a saturated CH_2Cl_2 solution. ^{1}H NMR (400 MHz, $CDCl_3$) δ 7.94 (d, $^3J_{HH}$ = 1.8 Hz, 1H, *H*C═CH Im), 6.83 (d, $^3J_{HH}$ = 1.8 Hz, 1H, HC═C*H* Im), 6.82–6.81 (m, 2H, $C_6H_2(CH_3)_3$), 5.33 (dd, $^2J_{HH}$ = 14.6 Hz, $^3J_{HH}$ = 3.0 Hz, 1H, CH_CH$_D$Im), 4.35 (app. s, 6H, 5 × C_5H_5 + C_5H_4S), 4.26 (m, 1H, C_5H_4S), 4.20 (m, 1H, C_5H_4S), 3.91 (dd, $^2J_{HH}$ = 14.2 Hz, $^3J_{HH}$ = 2.4 Hz, 1H, CH$_A$H$_B$S), 3.78 (td, $^2J_{HH}$ = $^3J_{HH}$ = 14.2 Hz, $^3J_{HH}$ = 3.7 Hz, 1H, CH$_C$H$_D$Im), 3.55 (td, $^2J_{HH}$ = $^3J_{HH}$ = 13.5 Hz, $^3J_{HH}$ = 4.2 Hz, 1H, CH_AH$_B$S), 3.34 (app. s, 1H, C_5H_4S), 2.29 (s, 3H, $C_6H_2(CH_3)_3$), 1.98 (s, 3H, $C_6H_2(CH_3)_3$), 1.76 (s, 3H, $C_6H_2(CH_3)_3$), 1.63 (s, 15H, $C_5(CH_3)_5$). ^{13}C NMR (100 MHz, $CDCl_3$) δ 166.29 (d, J_{CRh} = 54.3 Hz, N*C*N), 139.10, 138.61, 135.44, 133.57 (4 × C_{quat} $C_6H_2(CH_3)_3$), 129.16, 127.32 (2 × CH $C_6H_2(CH_3)_3$), 126.08, 124.75 (2 × HC═*C*H Im), 100.03 (d, J_{CRh} = 6.2 Hz, ($C_5(CH_3)_5$), 80.35 (C_{quat} C_5H_4S), 72.92 (CH C_5H_4S), 70.21 (5 × CH C_5H_5), 69.87, 69.02, 66.50 (3 × CH C_5H_4S), 50.03 (*C*H_2Im), 35.17 (*C*H_2S), 21.11, 20.08, 18.74 (3 × C_6H_2(*C*H_3)$_3$), 9.47 (C_5(*C*H_3)$_5$). MS (ESI$^+$) *m*/*z* 703.5 (M$^+$–BF_4, 100%). Elem. anal. $C_{34}H_{41}BClF_4FeN_2RhS$ (790.50): calc. C, 51.61; H, 5.23; N, 3.54; found C, 51.51; H, 5.16; N, 3.46%.

Ruthenium complex (5). Imidazolium salt **3b** (52.0 mg, 0.1 mmol), [Ru(*p*-cymene)Cl_2]$_2$ (54.0 mg, 0.088 mmol) and Ag_2O (13.6 mg, 0.059 mmol) were dissolved in dry CH_2Cl_2 (30 mL) and the Schlenk tube was protected from light. The mixture was heated at reflux for 40 h then filtered through Celite and the solvent was evaporated to *ca.* 2 mL. Excess hexane was added and the precipitate was filtered through Celite, rinsed with hexane and recovered by dissolving in CH_2Cl_2. The solid was further purified by column chromatography on neutral alumina (grade I, deactivated with 6–8%

H_2O; eluent: CH_2Cl_2/MeOH 95 : 5) to give an orange solid (67 mg, 85%). X-Ray quality crystals were obtained by layering a saturated $CDCl_3$ solution with methyl *tert*-butyl ether. ^{1}H NMR (500 MHz, $CDCl_3$) δ 7.56 (br s, 1H, *H*C=CH Im), 7.20 (br s, 1H, $C_6H_2(CH_3)_3$), 7.09 (br s, 1H, $C_6H_2(CH_3)_3$), 6.84 (br s, 1H, HC=C*H* Im), 5.51, 5.07, 4.97 (br s, 3 × 1H, C*H* *p*-cym), 4.87 (m, 1H, CH_2Im), 4.70–4.30 (m, *X* × 1H, C_5H_4), 4.47 (br s, 5 × 1H, C_5H_5), 3.71 (br s, 1H, C*H* *p*-cym), 2.69 (br s, 1H, $(CH_3)_2$C*H* *p*-cym), 2.44, 2.20, 1.98 (br s, 3 × 3H, $C_6H_2(CH_3)_3$), 1.81 (br s, 3H, CH_3 *p*-cym), 1.23, 0.95 (br s, 2 × 3H, $(CH_3)_2$CH *p*-cym). ^{13}C NMR (125.8 MHz, $CDCl_3$) δ 164.53 (N*C*N), 141.02, 137.90, 137.45, 135.45 (4 × C_{quat} $C_6H_2(CH_3)_3$), 129.74, 129.67 (2 × CH $C_6H_2(CH_3)_3$), 126.63, 122.67 (2 × HC=*C*H Im), 107.77, 103.52 (2 × C_{quat} *p*-cym), 97.68, 93.16, 88.51, 79.78 (4 × CH *p*-cym), 71.08 (C_5H_5), 71.5–68.0 (C_5H_4), 49.20 (CH_2Im), 33.69 (CH_2S), 29.51 ($(CH_3)_2CH$ *p*-cym), 24.77 ($(CH_3)_2$CH *p*-cym), 21.53 ($C_6H_2(CH_3)_3$), 20.41 ($(CH_3)_2$CH *p*-cym), 18.63, 18.62 ($C_6H_2(CH_3)_3$), 17.95 (CH_3 *p*-cym). MS (ESI$^+$) *m*/*z* 701 (M^+–BF_4, 100%).

X-Ray crystallography. A single crystal of each compound was mounted under inert perfluoropolyether at the tip of a cryoloop and cooled in the cryostream of an Agilent Technologies OD XCALIBUR 3 CCD diffractometer for **4** or a GEMINI EOS CCD diffractometer for **5**. Data were collected using the monochromatic MoKα radiation (λ = 0.71073). The structures were solved by direct methods (SIR97) [27] and refined by least-squares procedures on F^2 using SHELXL-97.[28] All H atoms attached to carbon were introduced in idealised positions and treated as riding on their parent atoms in the calculations. In compound **4**, the BF_4 was found to be disordered, and three orientations of *ca.* 81, 10 and 9% occupancy were identified. The geometries of all three orientations were optimised, the thermal parameters of adjacent equivalent atoms were restrained to be similar, and only the non-hydrogen atoms of the major occupancy orientation were refined anisotropically (the others were refined isotropically). The drawing of the molecules was realised with the help of ORTEP3.[29] Crystal data and refinement parameters: see footnote §. Selected bond distances and angles are given in Table 1. CCDC 816175 and 816176

Acknowledgements

The authors thank the CNRS, the Agence Nationale de la Recherche for a grant to A.L. (ANR-07-JCJC-0041) and the Institut National Polytechnique de Toulouse for a grant to R.P. and A.L. (Soutien à la Mobilité Internationale).

Notes and references

1 For selected books and recent reviews, see: S. Díez-González, N-*Heterocyclic Carbenes: From Laboratory Curiosities to Efficient Synthetic Tools*, RSC Publishing, Cambridge, UK, 2011; F. Glorius, N-*Heterocyclic Carbenes in Transition Metal Catalysis*, Springer-Verlag, Heidelberg, Germany, 2007; V. César, S. Bellemin-Laponnaz and L. H. Gade, *Chem. Soc. Rev.*, 2004, **33**, 619; F. E. Hahn and M. C. Jahnke, *Angew. Chem., Int. Ed.*, 2008, **47**, 3122; S. Díez-González, N. Marion and S. P. Nolan, *Chem. Rev.*, 2009, **109**, 3612; J. C. Y. Lin, R. T. W. Huang, C. S. Lee, A. Bhattacharyya, W. S. Hwang and I. J. B. Lin, *Chem. Rev.*, 2009, **109**, 3561; P. L. Arnold and I. J. Casely, *Chem. Rev.*, 2009, **109**, 3599.
2 For selected reviews, see: D. Enders, O. Niemeier and A. Henseler, *Chem. Rev.*, 2007, **107**, 5606; N. Marion, S. Díez-González and S. P. Nolan, *Angew. Chem., Int. Ed.*, 2007, **46**, 2988.
3 G. Gasser, I. Ott and N. Metzler-Nolte, *J. Med. Chem.*, 2011, **54**, 3; A. Kascatan-Nebioglu, M. J. Panzner, C. A. Tessier, C. L. Cannon and W. J. Youngs, *Coord. Chem. Rev.*, 2007, **251**, 884.
4 H. M. Lee, C. C. Lee and P. Y. Cheng, *Curr. Org. Chem.*, 2007, **11**, 1491; O. Kuhl, *Chem. Soc. Rev.*, 2007, **36**, 592; A. T. Normand and K. J. Cavell, *Eur. J. Inorg. Chem.*, 2008, 2781; A. John and P. Ghosh, *Dalton Trans.*, 2010, **39**, 7183.
5 Selected papers on S–NHC ligands: M. Bierenstiel and E. D. Cross, *Coord. Chem. Rev.*, 2011, **255**, 574, and references therein; C. Fliedel and P. Braunstein, *Organometallics*, 2010, **29**, 5614; C. Fliedel, A. Sabbatini and P. Braunstein, *Dalton Trans.*, 2010, **39**, 8820; C. Fliedel, G. Schnee and P. Braunstein, *Dalton Trans.*, 2009, 2474; A. Ros, M. Alcarazo, D. Monge, E. Álvarez, R. Fernández and J. M. Lassaletta, *Tetrahedron: Asymmetry*, 2010, **21**, 1557; S. J. Roseblade, A. Ros, D. Monge, M. Alcarazo, E. Alvarez, J. M. Lassaletta and R. Fernandez, *Organometallics*, 2007, **26**, 2570; A. Ros, D. Monge, M. Alcarazo, E. Alvarez, J. M. Lassaletta and R. Fernandez, *Organometallics*, 2006, **25**, 6039; H. V. Huynh, D. Yuan and Y. Han, *Dalton Trans.*, 2009, 7262; H. V. Huynh, C. H. Yeo and G. K. Tan, *Chem. Commun.*, 2006, 3833.
6 C. Gandolfi, M. Heckenroth, A. Neels, G. Laurenczy and M. Albrecht, *Organometallics*, 2009, **28**, 5112.
7 For ferrocene-containing NHC ligands, see: B. Bildstein, M. Malaun, H. Kopacka, K.-H. Ongania and K. Wurst, *J. Organomet. Chem.*, 1998, **552**, 45; H. Seo, H.-J. Park, B. Y. Kim, J. H. Lee, S. U. Son and Y. K. Chung, *Organometallics*, 2003, **22**, 618; K. S. Coleman, S. Gischig and A. Togni, *Organometallics*, 2004, **23**, 2479; S. Turberville, S. I. Pascu and M. L. H. Green, *J. Organomet. Chem.*, 2005, **690**, 653; D. M. Khramov, E. L. Rosen, V. M. Lynch and C. W. Bielawski, *Angew. Chem., Int. Ed.*, 2008, **47**, 2267; E. L. Rosen, C. D. Varnado, A. G. Tennyson, D. M. Khramov, J. W. Kamplain, D. H. Sung, P. T. Cresswell, V. M. Lynch and C. W. Bielawski, *Organometallics*, 2009, **28**, 6695; C. D. Varnado Jr, V. M. Lynch and C. W. Bielawski, *Dalton Trans.*, 2009, 7253; U. Siemeling, C. Färber and C. Bruhn, *Chem. Commun.*, 2009, 98.
8 P. D. Beer, P. A. Gale and Z. Chen, *Adv. Phys. Org. Chem.*, 1999, **31**, 1; A. Niemz and V. M. Rotello, *Acc. Chem. Res.*, 1998, **32**, 44.
9 For selected papers, see: C. Valério, J.-L. Fillaut, J. Ruiz, J. Guittard, J.-C. Blais and D. Astruc, *J. Am. Chem. Soc.*, 1997, **119**, 2588; A. Labande, J. Ruiz and D. Astruc, *J. Am. Chem. Soc.*, 2002, **124**, 1782; D. Astruc, C. Ornelas and J. Ruiz, *Acc. Chem. Res.*, 2008, **41**, 841; D. Astruc, E. Boisselier and C. Ornelas, *Chem. Rev.*, 2010, **110**, 1857.
10 A. M. Allgeier and C. A. Mirkin, *Angew. Chem., Int. Ed.*, 1998, **37**, 894; G. Liu, H. He and J. Wang, *Adv. Synth. Catal.*, 2009, **351**, 1610.
11 I. M. Lorkovic, R. R. Duff Jr. and M. S. Wrighton, *J. Am. Chem. Soc.*, 1995, **117**, 3617; C. K. A. Gregson, V. C. Gibson, N. J. Long, E. L. Marshall, P. J. Oxford and A. J. P. White, *J. Am. Chem. Soc.*, 2006, **128**, 7410; M. D. Sanderson, J. W. Kamplain and C. W. Bielawski, *J. Am. Chem. Soc.*, 2006, **128**, 16514; A. B. Powell, C. W. Bielawski and A. H. Cowley, *J. Am. Chem. Soc.*, 2009, **131**, 18232; A. G. Tennyson, V. M. Lynch and C. W. Bielawski, *J. Am. Chem. Soc.*, 2010, **132**, 9420; A. B. Powell, C. W. Bielawski and A. H. Cowley, *J. Am. Chem. Soc.*, 2010, **132**, 10184; A. G. Tennyson, R. J. Ono, T. W. Hudnall, D. M. Khramov, J. A. V. Er, J. W. Kamplain, V. M. Lynch, J. L. Sessler and C. W. Bielawski, *Chem.–Eur. J.*, 2010, **16**, 304.
12 T. B. Higgins and C. A. Mirkin, *Inorg. Chim. Acta*, 1995, **240**, 347; E. T. Singewald, X. Shi, C. A. Mirkin, S. J. Schofer and C. L. Stern, *Organometallics*, 1996, **15**, 3062; A. M. Allgeier and C. A. Mirkin, *Organometallics*, 1997, **16**, 3071; C. S. Slone, C. A. Mirkin, G. P. A. Yap, I. A. Guzei and A. L. Rheingold, *J. Am. Chem. Soc.*, 1997, **119**, 10743; X. Liu, A. H. Eisenberg, C. L. Stern and C. A. Mirkin, *Inorg. Chem.*, 2001, **40**, 2940; D. A. Weinberger, T. B. Higgins, C. A. Mirkin, C. L. Stern, L. M. Liable-Sands and A. L. Rheingold, *J. Am. Chem. Soc.*, 2001, **123**, 2503.

13 J. Wolf, A. Labande, J.-C. Daran and R. Poli, *Eur. J. Inorg. Chem.*, 2007, 5069.
14 S. Gülcemal, A. Labande, J.-C. Daran, B. Çetinkaya and R. Poli, *Eur. J. Inorg. Chem.*, 2009, 1806; N. Debono, A. Labande, E. Manoury, J.-C. Daran and R. Poli, *Organometallics*, 2010, **29**, 1879.
15 I. V. Kourkine, C. S. Slone, E. T. Singewald, C. A. Mirkin, L. M. Liable-Sands and A. L. Rheingold, *Inorg. Chem.*, 1999, **38**, 2758.
16 A. M. Allgeier, C. S. Slone, C. A. Mirkin, L. M. Liable-Sands, G. P. A. Yap and A. L. Rheingold, *J. Am. Chem. Soc.*, 1997, **119**, 550.
17 J. A. Mata, A. R. Chianese, J. R. Miecznikowski, M. Poyatos, E. Peris, J. W. Faller and R. H. Crabtree, *Organometallics*, 2004, **23**, 1253.
18 S. Saravanakumar, M. K. Kindermann, J. Heinicke and M. Koeckerling, *Chem. Commun.*, 2006, 640; D. M. Khramov, V. M. Lynch and C. W. Bielawski, *Organometallics*, 2007, **26**, 6042; D. Tapu, C. Owens, D. VanDerveer and K. Gwaltney, *Organometallics*, 2009, **28**, 270.
19 A. Kascatan-Nebioglu, M. J. Panzner, J. C. Garrison, C. A. Tessier and W. J. Youngs, *Organometallics*, 2004, **23**, 1928.
20 A. P. da Costa, M. Sanaú, E. Peris and B. Royo, *Dalton Trans.*, 2009, 6960; K. Ogata, T. Nagaya and S.-i. Fukuzawa, *J. Organomet. Chem.*, 2010, **695**, 1675.
21 M. Poyatos, A. Maisse-François, S. Bellemin-Laponnaz, E. Peris and L. H. Gade, *J. Organomet. Chem.*, 2006, **691**, 2713; R. Cariou, C. Fischmeister, L. Toupet and P. H. Dixneuf, *Organometallics*, 2006, **25**, 2126; X. Wang, S. Liu, L.-H. Weng and G.-X. Jin, *Chem.–Eur. J.*, 2007, **13**, 188; Y. Zhang, C. Chen, S. C. Ghosh, Y. Li and S. H. Hong, *Organometallics*, 2010, **29**, 1374; W. Ghattas, H. Müller-Bunz and M. Albrecht, *Organometallics*, 2010, **29**, 6782; W. N. O. Wylie, A. J. Lough and R. H. Morris, *Organometallics*, 2011, **30**, 1236.
22 F. H. Allen, *Acta Crystallogr., Sect. B: Struct. Sci.*, 2002, **B58**, 380.
23 For a comprehensive review on chemical redox agents, see: N. G. Connelly and W. E. Geiger, *Chem. Rev.*, 1996, **96**, 877.
24 The weak feature at 0.1 V is probably due to traces of oxygen. A second experiment carried out on the same sample in the range −1 V/+1.2 V showed no such feature but only the ferrocene/ferrocenium redox wave.
25 T. Sixt, M. Sieger, M. J. Krafft, D. Bubrin, J. Fiedler and W. Kaim, *Organometallics*, 2010, **29**, 5511.
26 A. G. Tennyson, D. M. Khramov, C. D. Varnado, P. T. Creswell, J. W. Kamplain, V. M. Lynch and C. W. Bielawski, *Organometallics*, 2009, **28**, 5142.
27 A. Altomare, M. C. Burla, M. Camalli, G. L. Cascarano, C. Giacovazzo, A. Guagliardi, A. G. G. Moliterni, G. Polidori and R. Spagna, *J. Appl. Crystallogr.*, 1999, **32**, 115.
28 G. M. Sheldrick, *Acta Crystallogr., Sect. A: Fundam. Crystallogr.*, 2008, **A64**, 112.
29 M. N. Burnett and C. K. Johnson, *ORTEPIII*, Report ORNL-6895, Oak Ridge National Laboratory, Oak Ridge, Tennessee, US, 1996; L. J. Farrugia, *J. Appl. Crystallogr.*, 1997, **30**, 565.

